

Topological Summation in Lattice Gauge Theory

Wolfgang Bietenholz¹ and Ivan Hip²

¹ Instituto de Ciencias Nucleares, Universidad Nacional Autónoma de México
A.P. 70-543, C.P. 04510 Distrito Federal, Mexico

² Faculty of Geotechnical Engineering, University of Zagreb
Hallerova aleja 7, 42000 Varaždin, Croatia

E-mail: wolbi@nucleares.unam.mx

Abstract. In gauge theories the field configurations often occur in distinct topological sectors. In a lattice regularised system with chiral fermions, these sectors can be defined by referring to the Atiyah-Singer Index Theorem. However, if such a model is simulated with local updates of the lattice gauge configuration, the Monte Carlo history tends to get stuck in one sector for many steps, in particular on fine lattices. Then expectation values can be measured only within specific sectors. Here we present a pilot study in the 2-flavour Schwinger model which explores methods of approximating the complete result for an observable — corresponding to a suitable sum over all sectors — based on numerical measurements in a few specific topological sectors. We also probe various procedures for an indirect evaluation of the topological susceptibility, starting from such topologically restricted measurements.

1. Topological sectors in gauge theories

Our general framework in this article is the functional integral formulation of quantum physics in Euclidean space. In this setting, the set of configurations may occur in disjoint subsets, so that all continuously deformed configurations belong to the same subset. Such subsets are known as *topological sectors*. Continuous deformations capture all configurations in one topological sector, but none of any different sector (general aspects are discussed *e.g.* in Refs. [1]).

The simplest example where this situation occurs is a quantum mechanical scalar particle moving on the circle S^1 , with periodic boundary conditions in Euclidean time. The expectation value of some observable \mathcal{O} in this system is given by

$$\langle \mathcal{O} \rangle = \frac{1}{Z} \int \mathcal{D}\varphi \mathcal{O}[\varphi] \exp(-S[\varphi]) , \quad \text{where} \quad Z = \int \mathcal{D}\varphi \exp(-S[\varphi]) \quad (1)$$

is the partition function, and $\mathcal{D}\varphi$ is the sum over all closed paths $\varphi(t) \in S^1$ in some period T , *i.e.* $t \in [0, T]$ and $\varphi(0) = \varphi(T)$. The set of all these paths is naturally divided into disjoint subsets, which are characterised by the winding number

$$Q = \frac{1}{2\pi} \int_0^T dt \dot{\varphi} \in \mathbb{Z} , \quad (2)$$

which represents in this case the *topological charge*. Continuous path deformations cannot change Q , hence these subsets are indeed topological sectors.

Topological sectors also occur in a variety of gauge theories [1]. Let us consider gauge configurations in a Euclidean space with periodic boundary conditions (a torus). If they are split into topological sectors, the characteristic topological charge Q is also denoted as the Pontryagin index. Two examples are

$$\begin{aligned} 2\text{d } U(1) & : Q = \frac{1}{\pi} \int d^2x \epsilon_{\mu\nu} F_{\mu\nu}(x) , \\ 4\text{d } SU(3) & : Q = \frac{1}{32\pi^2} \text{Tr} \int d^4x F_{\mu\nu}(x) \tilde{F}_{\mu\nu}(x) , \end{aligned} \quad (3)$$

where $F_{\mu\nu}$ is the field strength tensor, and $\tilde{F}_{\mu\nu} := \epsilon_{\mu\nu\rho\sigma} F_{\rho\sigma}$. Gauge configurations can be continuously deformed only within a fixed topological sector, hence the functional integral splits into separate integrals for each $Q \in \mathbb{Z}$.

Let us now address such a gauge theory in the presence of *chiral fermions*, *i.e.* massless fermions with a Dirac operator D that anti-commutes with γ_5 , $D\gamma_5 + \gamma_5 D = 0$. In this case the zero modes of the Dirac operator have a definite chirality ± 1 .

For such a Dirac operator, in a given gauge background, we denote the number of zero modes with chirality $+1$ (-1) as n_+ (n_-). Their difference is the *fermion index*

$$\nu := n_- - n_+ \in \mathbb{Z} . \quad (4)$$

The *Atiyah-Singer Index Theorem* [2] states that for any gauge configuration, this index coincides with the topological charge

$$Q \stackrel{!}{=} \nu . \quad (5)$$

2. Lattice regularisation

The lattice regularisation reduces the (Euclidean) space to discrete sites x , which are separated by some finite lattice spacing a . The latter implies an UV regularisation of the corresponding quantum field theory. Matter field variables are now defined on each lattice site, *e.g.* $\bar{\Psi}_x$, Ψ_x for fermion fields, while gauge fields can be formulated as *compact link variables* $U_{x,\mu} \in \{\text{gauge group}\}$. It is a great virtue that this formulation is *gauge invariant* even on the regularised level, so in this approach no gauge fixing is needed.

A priori there are *no* topological sectors anymore in the lattice regularised system; all configurations can now be continuously deformed into each other. Still, the desired connection to the continuum theory motivates the attempt to introduce somehow (the analogue of) topological sectors also on the lattice. A number of suggestions appeared in the literature, often with a somewhat questionable conceptual basis. A clean formulation emerged only at the very end of the last century, based on chiral lattice fermions. Their lattice Dirac operator D cannot simply anti-commute with γ_5 due to the notorious doubling problem of lattice fermions [3], but it may obey the *Ginsparg-Wilson Relation* (GWR), which reads (in its simplest form)

$$D\gamma_5 + \gamma_5 D = aD\gamma_5 D . \quad (6)$$

This still guarantees a lattice deformed — but exact — version of the chiral symmetry [4]. The latter also implies that the corresponding lattice Dirac operator has exact zero modes with a

definite chirality, as in the continuum. Hence we can adopt the Index Theorem [5] and define the topological charge of a lattice gauge configuration as $Q := \nu$.

We remark that random lattice gauge configurations always occur with $n_+ = 0$ or $n_- = 0$; configurations with a cancellation in the lattice fermion index also exist (the free fermion is an example), but their probability measure seems to vanish.¹

3. Monte Carlo simulation

Observables in quantum gauge theory can be evaluated beyond perturbation theory by means of Monte Carlo simulations. The idea is to use a sizeable set of gauge configurations $[U]$ (consisting of link variables all over the lattice volume), which are generated randomly with the probability distribution

$$p[U] = \det D[U] \exp(-S_{\text{gauge}}[U]) . \quad (7)$$

Here we assume a fermion action, which is bilinear in the Grassmann valued spinor fields $\bar{\Psi}, \Psi$. Their functional integration $\mathcal{D}\bar{\Psi}\mathcal{D}\Psi$ is carried out already, giving rise to the fermion determinant $\det D[U]$.

The summation over this set of configurations yields a numerical measurement of expectation values $\langle \dots \rangle$, in particular of n -point functions. These results obviously come with some statistical error (since the available set of configurations is finite), and a systematic error (*e.g.* due to the finite lattice spacing a , which usually requires a continuum extrapolation). Both can be estimated and reduced if necessary by extended simulations. On the other hand, we stress again that the result is fully *non-perturbative*; we deal with the complete action in the exponent, *i.e.* we capture directly the given model at finite interaction strength.

Practical algorithms for the generation of gauge configurations (with the given probability distribution) perform local updates, *i.e.* in one step a configuration is modified just locally. Iterating such steps many times leads to a (quasi-)independent new configuration, to be used for the next measurement. Changing a gauge configuration drastically in a single step is also conceivable in principle, but in practice such algorithms tend to be inefficient.²

A problem with a sequence of local updates is, however, that it hardly ever changes the topological sector — although one should do so frequently in order to sample correctly the entire space of configurations. This problem is particularly striking in the attempts to simulate QCD with chiral quarks; the JLQCD Collaboration performed very extensive 2-flavour QCD simulations of this kind [6] — which led to interesting results — but the Monte Carlo histories were always confined to the trivial topological sector of charge $Q = 0$.

Most QCD simulations with dynamical quarks involve a non-chiral lattice quark formulation, since Ginsparg-Wilson fermions are tedious to simulate. In particular Wilson fermions (and variants thereof) have the disadvantage of additive mass renormalisation, but the problem with sampling the topological sectors is less severe so far. However, that property depends on the lattice spacing; typical values that have been used in the past are $a \approx 0.05 \dots 0.1$ fm. Once one tries to proceed to even finer lattices, the problem of confinement of the Monte Carlo history to a single topological sector is expected to show up also in this formulation [7].³

¹ The same holds for the specific lattice field configurations which are exactly *on* a topological boundary, so we can ignore them.

² Cluster algorithms are a counter example for certain spin models, but no efficient application to lattice gauge theories is known so far.

³ To be more explicit: any algorithm has to obey “detailed balance”, *i.e.* the transition probabilities of some configuration C_1 to C_2 and vice versa have to match the probability ratio for these configurations to occur

So we have to address the question how to handle Monte Carlo simulations if the history tends to be trapped for a very long (computing) time, *i.e.* for many, many update steps, in *one* topological sector. What are then the prospects for measuring some n -point function, or the topological susceptibility

$$\chi_t := \frac{1}{V} \left(\langle Q^2 \rangle - \langle Q \rangle^2 \right) \quad (V = \text{volume}) , \quad (8)$$

which actually require the summation over a variety of topological sectors, with suitable statistical weights?

This is a delicate and highly relevant issue. Here we address it in a toy model study of the 2-flavour Schwinger model, which we simulated [8] with *dynamical overlap hypercube fermions*; this is one version of chiral lattice fermions [9], with a Dirac operator that solves the GWR (6).⁴ We designed and applied a variant of the Hybrid Monte Carlo algorithm, which is particularly suitable for this type of lattice fermions [8].

4. The Schwinger model

The Schwinger model [11] represents Quantum Electrodynamics on a plane (QED₂). It is a popular toy model; in particular it shares with QCD the property of fermion confinement [12] (although the gauge group is Abelian) and the presence of topological sectors, see eq. (3). On the other hand there are qualitative differences, such as the absence of a running gauge coupling in the Schwinger model. In the continuum its Lagrangian can be written as

$$\mathcal{L}(\bar{\Psi}, \Psi, A_\mu) = \bar{\Psi}(x) \left[\gamma_\mu (i \partial_\mu + g A_\mu(x)) + m \right] \Psi(x) + \frac{1}{2} F_{\mu\nu}(x) F_{\mu\nu}(x) . \quad (9)$$

We are interested in the case of $N_f = 2$ degenerate fermion flavours of mass $m \ll g$, where Ref. [13] made the following predictions:

$$\text{chiral condensate} \quad \Sigma := -\langle \bar{\Psi} \Psi \rangle = 0.388 \dots (mg^2)^{1/3} , \quad (10)$$

$$\text{pion mass} \quad M_\pi = 2.008 \dots (m^2 g)^{1/3} . \quad (11)$$

As in 2-flavour QCD, a “meson” singlet and a triplet emerge, the former (latter) being massive (massless) in the chiral limit $m \rightarrow 0$, cf. eq. (11). Referring to this analogy, and in agreement with the literature, we denote the triplet as “pions”. Its emergence in 2 dimensions might appear somewhat surprising; the theoretical background of these “quasi-Nambu-Goldstone bosons” was first discussed in Ref. [14].

5. Numerical measurement at fixed topology

We simulated the 2-flavour Schwinger model at $\beta := 1/g^2 = 5$ [8]. This implies smooth gauge configurations (mean plaquette value $\simeq 0.9$). Also the “meson” dispersion relations confirm that lattice artifacts are tiny [8], hence we can confront our results directly with the continuum predictions (10), (11), without really needing a continuum extrapolation. On the other hand, finite size effects are significant, and they are in fact necessary for our discussion of topology dependent observables. We simulated on $L \times L$ lattices of sizes $L = 16, 20, 24, 28, 32$ with

(Boltzmann weights), $p(C_1 \rightarrow C_2)/p(C_2 \rightarrow C_1) = \exp(S[C_1] - S[C_2])$. The boundaries between topological sectors are surrounded by zones of high action, *i.e.* low probability. As the lattice spacing a is reduced, their weight $p(C)$ decreases with a high power of a [7]. Hence a sequence of small update steps will rarely tunnel through such a boundary.

⁴ In this formulation we insert an improved kernel into the overlap formula, instead of the Wilson kernel of the standard overlap operator [10]. The virtues include an improved locality and scaling behaviour, and approximate rotation symmetry [9].

L	m	number of configurations				topological transitions
		$\nu = 0$	$ \nu = 1$	$ \nu = 2$	total	
16	0.01	2428	307		2735	7
16	0.03	1070	508		1578	2
16	0.06	741	660		1401	7
16	0.09	919	587	1	1507	7
16	0.12	664	501	248	1413	8
16	0.18	791	563	50	1404	15
16	0.24	576	978	56	1637	17
L	m	number of configurations				total
		$\nu = 0$	$ \nu = 1$	$ \nu = 2$	$ \nu = 3$	
20	0.01	435	304			739
24	0.01			278	273	551
28	0.01		240		180	420
32	0.01	138	98	82		318
32	0.06	91	293			384

Table 1. Statistics for lattice size $L = 16$ (above) and $L > 16$ (below) and various fermion masses m , in distinct topological sectors (ν is the fermion index). Multiple starts of Monte Carlo histories were necessary to get access to various topological sectors, since topological transitions were very rare.

fermion masses in the range $m = 0.01 \dots 0.24$ (in lattice units). Our statistics is displayed in Table 1.

Let us first address the *Dirac spectrum*. All the eigenvalues of a lattice Dirac operator (before adding the mass), which obeys the GWR (6), are located on the circle in the complex plane with centre and radius $1/a$, as illustrated in Fig. 1. This confirms that the zero modes are exact,

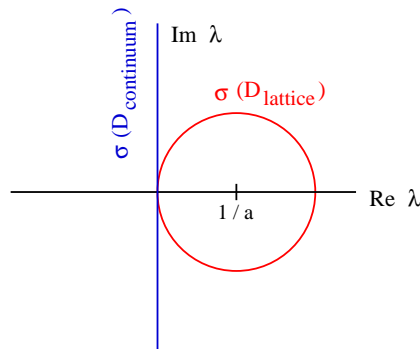


Figure 1. The spectrum of a lattice Dirac operator that fulfils the GWR (6) is located on a circle in the complex plane. In the continuum limit $a \rightarrow 0$ it turns into the imaginary axis.

and we have mentioned before that their fermion index is identified with the topological charge, $Q = \nu = n_- - n_+$.⁵

In this study we could evaluate the complete Dirac spectrum for our lattice configurations

⁵ Actually throughout this study only the absolute value $|\nu|$ matters.

(which is not feasible in 4 dimensions, except for tiny lattices). To make this spectrum compatible with the continuum formulation, we map it stereographically onto the imaginary axis [15]. Based on the eigenvalues λ_i that we obtain after this mapping, we obtain the *chiral condensate*

$$\Sigma := -\langle \bar{\Psi}\Psi \rangle = \frac{1}{V} \left\langle \sum_i \frac{1}{|\lambda_i| + m} \right\rangle. \quad (12)$$

The sum can be computed for each configuration, but expectation values can only be measured within fixed topological sectors. Table 1 shows that topological transitions are indeed so rare that the entire space of configurations is not well sampled, but specific sectors are explored well. Hence we measure results for the expectation values of the chiral condensate at specific values of $|\nu|$,

$$\Sigma_{|\nu|} = -\langle \bar{\Psi}\Psi \rangle_{|\nu|} = \frac{1}{V} \left\langle \sum_i \frac{1}{|\lambda_i| + m} \right\rangle_{|\nu|} := \frac{|\nu|}{mV} + \varepsilon_{|\nu|}. \quad (13)$$

In the last expression we split off the zero mode contribution to $\Sigma_{|\nu|}$, which dominates at small mass m (and $\nu \neq 0$), and we denote the rest as $\varepsilon_{|\nu|}$. Numerical results are shown in Fig. 2.

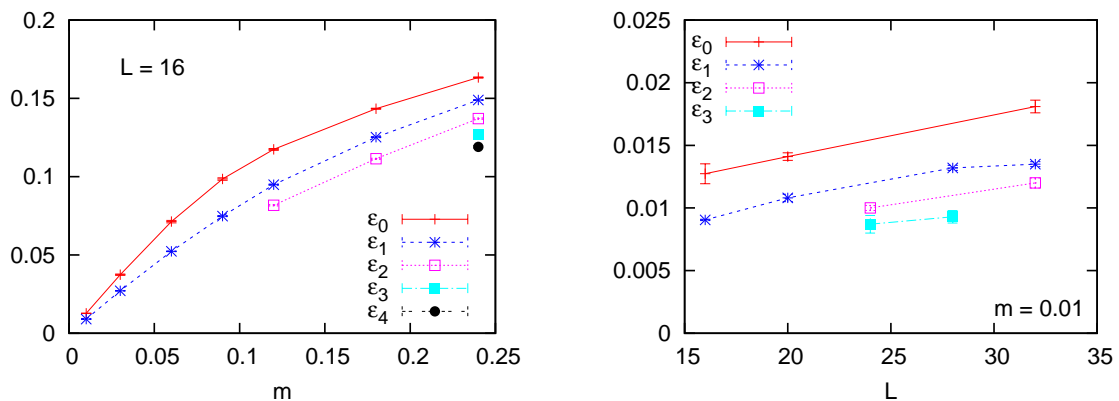


Figure 2. Numerical results for the chiral condensate at $|\text{topological charge}| = |\nu|$, after subtracting the zero mode contribution, cf. eq. (13), at $L = 16$ (on the left) and at $m = 0.01$ (on the right).

It is a generic property of stochastic Hermitian matrices (such as $\gamma_5 D$) that zero eigenvalues repel the low-lying non-zero modes. This suggests the inequality

$$\varepsilon_0 > \varepsilon_1 > \varepsilon_2 \dots \quad (14)$$

at fixed m and V , which is confirmed consistently by the plot in Fig. 2 on the left. Moreover the plot on the right shows that

$$\varepsilon_i(V_1) > \varepsilon_i(V_2) \quad \text{for} \quad V_1 > V_2, \quad (15)$$

which is less obvious: in a larger volume more eigenvalues cluster near zero, which supersedes the pre-factor $1/V$.

The rest of this article is devoted to tests of three different methods for approximately extracting “physical” quantities (*i.e.* quantities which are properly summed over all topological sectors), based on measurements in a few specific sectors.

6. Gaussian evaluation of the topological susceptibility

We first assume a Gaussian distribution of the topological charges — this is certainly reasonable, for instance precision tests in $SU(3)$ pure gauge theory revealed at most tiny deviations from this behaviour [16]. It implies that the chiral condensate is composed as

$$\Sigma = \sum_{\nu=-\infty}^{\infty} p(|\nu|) \Sigma_{|\nu|} \quad , \quad p(|\nu|) = \frac{\exp\{-\nu^2/(2V\chi_t)\}}{\sum_{\nu} \exp\{-\nu^2/(2V\chi_t)\}} \quad (16)$$

Parity symmetry assures that $\langle \nu \rangle = 0$, hence the topological susceptibility simplifies to

$$\chi_t = \frac{\langle \nu^2 \rangle}{V} \quad (17)$$

In most volumes we have data for $\Sigma_0 \dots \Sigma_Q$, *i.e.* up to some maximal topological charge Q . Thanks to inequality (14) all the higher charge contributions — for $|\nu| > Q$ — are bounded as

$$\frac{|\nu|}{mV} < \Sigma_{|\nu|} < \frac{|\nu|}{mV} + \varepsilon_Q \quad (18)$$

Hence for a given value of the susceptibility χ_t the sum in eq. (16) can be performed, up to a uncertainty which affects Σ only mildly, since $\Sigma_{|\nu|}$ for high charges contribute only little.

In two volumes, $L = 24$ and 28 , some $\Sigma_{|\nu|}$ data are missing for $|\nu| < Q$ (see Table 1); in these cases we can again fix a minimal and a maximal value for $\varepsilon_{|\nu|}$, this time based on inequality (15) and the results in the next smaller and next larger volume.

So we can probe any ansatz for χ_t and compute the corresponding value of Σ up to a modest uncertainty. We require the result to agree (within errors) with the prediction (10). In this way we determine χ_t . Fig. 3 shows the results for $L = 16$ and $m = 0.01, 0.03, 0.06$ — for higher masses the assumption $m \ll g \simeq 0.45$, which is needed for the prediction (10), seems to fail. Since the theory refers to infinite volume, we expect the result to improve for increasing m (*i.e.* for shorter correlation length) within the allowed range.

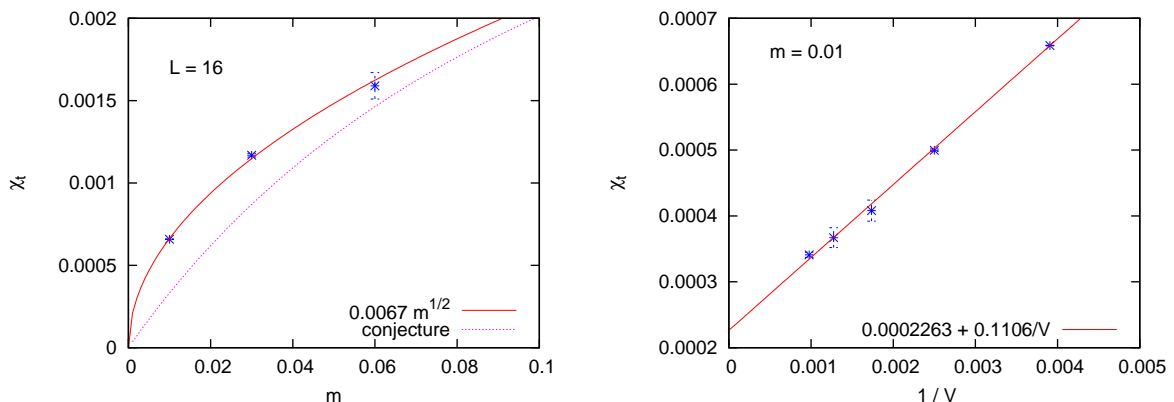


Figure 3. Our results for the topological susceptibility χ_t based on Gaussian summation. On the left: in a fixed volume $V = 16^2$ our data are compatible with an interpolation $\chi_t(m) \propto \sqrt{m}$, and for increasing mass (*i.e.* reduced finite size effects) we approach the conjecture (19). On the right: at fixed $m = 0.01$ we obtain results for χ_t , which seem to follow a behaviour linear in $1/V$.

The result is compared to a QCD-inspired conjecture of Ref. [17] (for N_f flavours, in a large volume),

$$\frac{1}{\chi_t} = \frac{N_f}{m} \Sigma(N_f = 1, m = 0) + \frac{1}{\chi_t(N_f = 0)}. \quad (19)$$

The first ingredient has been computed analytically, $\Sigma(N_f = 1, m = 0) \simeq 0.16g$ [14], and the quenched susceptibility $\chi_t(N_f = 0) \simeq 0.000332$ has been measured numerically [18]. Fig. 3 confirms that the corresponding curve approaches the fit through our values for increasing m .

Alternatively we fix the mass $m = 0.01$ and compare the results for $L = 16 \dots 32$ (plot in Fig. 3 on the right). In our largest volume, $V = 32^2$, we obtained $\chi_t = 0.000341(4)$, which is close to the value given by conjecture (19), $\chi_t = 0.000332$. An infinite volume extrapolation of our data, however, leads to a smaller susceptibility of $\chi_t = 0.000226(5)$.

7. Correlation of the topological charge density

A drawback of the method in Section 6 is that a known reference quantity is needed (here it was Σ), and results in various topological sectors are required. This is not the case for an approach suggested in Ref. [19], which derived a “model independent formula” for the *correlation of the topological charge density* ρ_t in one sector,

$$\lim_{|x| \rightarrow \infty} \langle \rho_t(x) \rho_t(0) \rangle_{|\nu|} \simeq -\frac{1}{V} \chi_t + \frac{\nu^2}{V^2} + O(V^{-3}). \quad (20)$$

For tests in 2-flavour QCD we refer to Ref. [20]. (The original formula even includes a correction for a possible deviation from a Gaussian distribution of the topological charges, which we neglect.) In order to justify the assumptions in the derivation of this formula, we have to assume a large expectation value $\langle \nu^2 \rangle = V \chi_t$, and a small ratio $|\nu|/\langle \nu^2 \rangle$.

As an example, we show in Fig. 4 the corresponding correlation at $L = 16$, $\nu = 0$ and various masses. Numerically the density was computed from the simplest lattice version of $\rho_t = \epsilon_{12} F_{12}$ (this is not problematic in the current setting, where we are always dealing with smooth configurations).

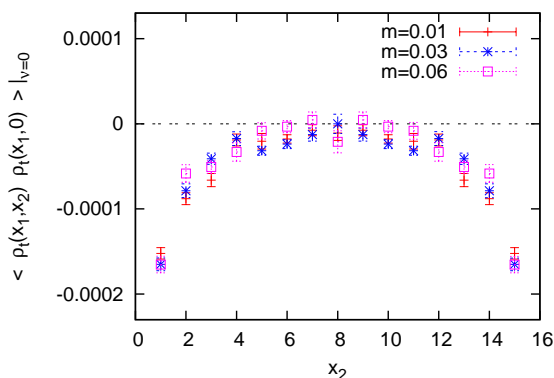


Figure 4. The correlation of the topological charge density for $L = 16$, $\nu = 0$ and $m = 0.01, 0.03, 0.06$. The statistical noise does not allow us to resolve a plateau value at large distances — overcoming this problem would require a huge statistics.

At large distances one should find a plateau value, which would then yield χ_t . In particular for $m = 0.06$, where the maximal distance might be sufficient to see the asymptotic behaviour,

we expect (based on the data and the conjectured formula in Section 6) a plateau value of $\chi_t/V \approx -6 \cdot 10^{-6}$. However, our statistical errors are of $O(10^{-5})$, so in order to clearly resolve this plateau we would need about 50 000 to 100 000 configurations (cf. Table 1). We conclude that the applicability of this method requires unfortunately a very large statistics.

8. Approximate topological summation of observables

We now proceed to the main approach in this study. It is a method that does not require a known input observable either (as in Section 7), but measurements in various topological sectors and volumes are needed. In fact this is the input which is usually accessible. Then one tries to extract a (topologically summed) observable $\langle O \rangle$ by employing the approximation formula

$$\langle O \rangle_{|\nu|} \approx \langle O \rangle + \frac{c}{V\chi_t} \left(1 - \frac{\nu^2}{V\chi_t} \right) \quad (c = \text{const.}) . \quad (21)$$

This formula has been derived first for the pion mass in QCD [21], but it applies generally to observables in a field theory with topology [8]. As in Section 7 one assumes a Gaussian distribution of the topological charges, and a large value of $V\chi_t$, as well as a small ratio $|\nu|/\langle \nu^2 \rangle$, are favourable for the validity of the approximations involved in the derivation. This approximation formula could be truly powerful in QCD and elsewhere, but it has never been tested before.

8.1. Application to the chiral condensate

Let us apply formula (21) to the chiral condensate. It is convenient to modify the notation,

$$\Sigma_\nu \approx \Sigma - \frac{A}{V} + \nu^2 \frac{B}{V^2} , \quad A = -\frac{c}{\chi_t} , \quad B = -\frac{c}{\chi_t^2} . \quad (22)$$

The unknown quantities are Σ , A and B , and we are ultimately interested in Σ and $\chi_t = A/B$. They can be determined (in the framework of this approximation) by numerical results for some Σ_ν :

- At fixed m and V , we can determine B , for instance from Σ_0 and Σ_1 .
- If we keep m fixed but consider two volumes, $V_1 \neq V_2$, we can further determine A , *e.g.* based on Σ_0 .

In total, it takes (at least) three Σ_ν values, involving two volumes, to obtain results for Σ and χ_t .

We follow this sequence of steps and start with the determination of B . If we use as our input the measurements in the topological sectors with $|\nu| = k, \ell$ (at fixed m and V), we denote the result as $B_{k,\ell}$,

$$\frac{1}{V} B_{k,\ell} = V \frac{\Sigma_k - \Sigma_\ell}{k^2 - \ell^2} = \frac{1}{m(k + \ell)} + V \frac{\varepsilon_k - \varepsilon_\ell}{k^2 - \ell^2} . \quad (23)$$

The semi-classical term, $1/(m(k + \ell))$, tends to vary strongly for different choices of k and ℓ . Ideally the quantum effects should render the results for $B_{k,\ell}$ similar again. As an example, we show in Fig. 5 results for $B_{k,0}$ at $L = 16$, $m = 24$. In fact the non-perturbative results are much more stable in k than the semi-classical contributions alone. Hence the first consistency test is passed well.

We proceed to the determination of A , and therefore of Σ , based on Σ_0 measurements in two volumes with sizes (L_1, L_2) . Here we consider $m = 0.01$ and we give two examples:

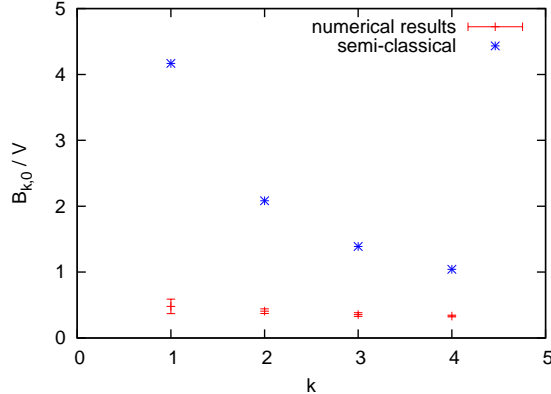


Figure 5. Results for the auxiliary variables $B_{k,0}$ (cf. eqs. (22), (23)) at $L = 16$, $m = 0.24$, for $k = 1, \dots, 4$. We see that the numerical results are quite consistent, in contrast to the semi-classical values.

- The Σ_0 values in $(L_1, L_2) = (16, 32)$ yield $\Sigma = 0.0199(7)$.
- The Σ_0 values in $(L_1, L_2) = (20, 32)$ yield $\Sigma = 0.0207(12)$.

Thus the consistency looks fine again, but these results are far below the prediction (10), $\Sigma = 0.04888$ (in an infinite volume). In this case, our results are strongly affected by finite size effects, which is not surprising: for the given fermion mass, the correlation length in infinite volume (given by eq. (11)) would be $\xi = 1/M_{\pi, V=\infty} \simeq 14$. The relatively small boxes enhance the Dirac eigenvalues $|\lambda_i|$, such that Σ decreases.

So the mass $m = 0.06$ should be more promising, where theory predicts $\xi \simeq 4.3$. Here we only have data in $(L_1, L_2) = (16, 32)$, for $|\nu| = 0, 1$, so we cannot repeat the above consistency tests. Nevertheless we can evaluate $\chi_t = 0.00118(30)$ (which is just compatible with the conjecture (19), $\chi_t \simeq 0.00146$). We further insert our most reliable result for B , namely $B_{1,0}$ measured in $L = 32$, and arrive at a result for Σ , which is indeed close to the theoretical prediction (11),

$$\Sigma_{\text{numerical}} = 0.0883(69) \quad , \quad \Sigma_{\text{theory}} = 0.0888 \quad . \quad (24)$$

8.2. Application to the pion mass

Let us also test the approximate summation formula (21) by applying it to the pion mass. As we mentioned before, this was the original idea of Ref. [21] (though that work referred to QCD). We re-write approximation (21) in the notation analogous to (22),

$$M_{\pi, |\nu|} \approx M_\pi - \frac{A}{V} + \frac{B}{V^2} \nu^2 \quad . \quad (25)$$

However, we now adopt a strategy which differs from the previous consideration of Σ : at fixed m we determine the three unknown parameters A , B , M_π directly by a least-square fit for some set of numerical $M_{\pi, |\nu|}$ values.

- For $m = 0.01$ we have in total 11 measurements of $M_{\pi, |\nu|}$ (see Table 1), and we include the most promising ones. We need at least two volumes, so we take the largest two with

$(L_1, L_2) = (28, 32)$. Moreover we only include the topological sectors with $|\nu| \leq 1$, which are favourable for the condition that $|\nu|/\langle\nu^2\rangle$ should be small. This leads to

$$\left. \begin{array}{l} L = 28 : \quad M_{\pi,0} \quad M_{\pi,1} \\ L = 32 : \quad 0.05(1) \quad 0.160(8) \end{array} \right\} \xrightarrow{\text{fit}} M_{\pi} = 0.073(25) , \quad (26)$$

which matches well the theoretical prediction, $M_{\pi} = 0.071$ (albeit with a large error).

• We proceed to $m = 0.06$, where we only have data for $(L_1, L_2) = (16, 32)$. Hence we have less choice in this case, but the finite size effects are less severe. Again we include the results for $|\nu| \leq 1$, which corresponds to four input measurements this time, and we arrive at

$$\left. \begin{array}{l} L = 16 : \quad M_{\pi,0} \quad M_{\pi,1} \\ L = 32 : \quad 0.041(1) \quad 0.271(4) \\ L = 32 : \quad 0.23(1) \quad 0.232(7) \end{array} \right\} \xrightarrow{\text{fit}} M_{\pi} = 0.233(8) . \quad (27)$$

Also this result agrees well with the theoretical pion mass, $M_{\pi} = 0.235$, and this time also the uncertainty is modest.

9. Conclusions

We have addressed a quite generic problem of lattice simulations in gauge theories with dynamical (quasi-)chiral fermions. The Monte Carlo histories of such simulations tend to get trapped in *one* topological sector for a very long (simulation) time, *i.e.* over many update steps of the lattice gauge configuration. A conceptual issue that one has to address in this situation is *ergodicity*, a property which is compulsory for a correct algorithm. Here we studied a more practical question: how can we evaluate the expectation value of some observable $\langle O \rangle$, when only numerical measurements restricted to a few topological sectors, $\langle O \rangle_{\nu}$, are available?

The dominant subject in contemporary lattice simulations is QCD with dynamical quarks. Here the problem of topological restriction is most striking when one deals with chiral lattice quarks (of overlap [10] or Domain Wall [22] type), which solve the Ginsparg-Wilson Relation (eq. (6) or generalisations thereof). The use of Wilson type quarks is more widespread because they are much faster to simulate, though plagued by additive mass renormalisation and problems related to operator mixing.^{6 7}

Here the aforementioned topological problem is less severe so far, but it is expected to show up as well when simulations will be carried out on finer and finer lattices, say with lattice spacing $a < 0.05$ fm. This renders the lattice QCD formulation more and more continuum-like, which is in general welcome, but it also makes it more difficult to change the topological sector.

This problem is not manifest in a very large volume, where $\langle O \rangle_{\nu}$ is the same for all indices ν (this property agrees with approximations (20), (21)). However, to suppress the topological dependence and other finite size effects, the volume has to be large compared to the correlation

⁶ Also that problem is avoided by the use of Ginsparg-Wilson fermions [23].

⁷ For completeness we add that “staggered fermions” are widespread as well in lattice QCD. They are also quick to simulate, and they do not suffer from additive mass renormalisation, but the number of flavours is not flexible. Therefore it is now popular to take the fourth root of the fermion determinant (cf. eq. (7)), which formally corresponds to a single flavour, but this is harmful for locality, which is conceptually important. The question if this is a reason to worry in practice is highly controversial. In any case, neither Wilson nor staggered fermions do provide a sound definition of the topological charge since there is no well-defined fermion index, in contrast to Ginsparg-Wilson fermions [5]. Hence one has to refer to some rather hand-waving definition in these cases.

length, which is given by the inverse pion mass, $\xi_{\text{QCD}} \approx 1.4 \text{ fm} \ll La$. But when a is very small, this requires a huge lattice size L , which makes simulations again very tedious.

As a way out, the use of open boundary conditions in the Euclidean time direction has recently been advocated, so that topological charge can gradually flow in or out of the volume during a simulation [24]. In our study, however, we stay with periodic boundary conditions for the gauge fields, which guarantee that the topological charge is always integer, along with (discrete) translation invariance. As a toy model we considered the Schwinger model with two light, degenerate flavours, which were represented on the lattice by dynamical overlap hypercube fermions. In a set of small or moderate volumes, this only enabled measurements inside some specific topological sectors. In order to establish a link to the “physical” quantities, we tested three methods to approximate the topological summation:

- The confrontation of a Gaussian summation with a known observable allows us to fix the topological susceptibility χ_t . This method is robust, but it requires a known input quantity. This is available in the 2-flavour Schwinger model [13] (we used the chiral condensate), but not in general.
- Next we tested a method to evaluate χ_t based on the correlation function of the topological charge density [19]. More precisely, one searches for an asymptotic plateau of this correlation at large distances, which should amount to $-\chi_t/V$ (at $\nu = 0$). Unfortunately this value tends to be tiny for realistic settings, hence its resolution requires a very large statistics.
- Our main goal was the test of an approximate summation formula given in Ref. [21], which could provide a “physical” result $\langle O \rangle$, using only measurements of some topologically restricted observables $\langle O \rangle_\nu$ as an input — for various values of $|\nu|$, in at least two volumes. This method is potentially powerful, but it has never been tested before. Our results suggest that it may work, if the assumptions used in the derivation of this formula are reasonably well justified. In particular, $V\chi_t = \langle \nu^2 \rangle$ should be “large”, but it is difficult to predict explicitly what this means. In our settings this quantity was always below 0.5, but nevertheless we found decent (though not very precise) results for the topologically summed chiral condensate and pion mass. This observation is encouraging for applications in QCD simulations with dynamical quarks.

Acknowledgements: Stanislav Shcheredin and Jan Volkholz have contributed to this work at an early stage. We also thank Poul Damgaard, Stephan Dürr, Hidenori Fukaya and Jim Hetrick for helpful comments. This work was supported by the Croatian Ministry of Science, Education and Sports (project 0160013) and by the Deutsche Forschungsgemeinschaft through Sonderforschungsbereich Transregio 55 (SFB/TR55) “Hadron Physics from Lattice QCD”.

References

- [1] Polyakov A M 1987 *Gauge Fields and Strings* (Harwood Academic Publishers)
Rajaraman R 1987 *Solitons and Instantons* (North-Holland Personal Library)
Coleman S 1988 *Aspects of Symmetry* (Cambridge University Press)
- [2] Atiyah M F and Singer I M 1968 *Ann. Math.* **87** 484
- [3] Nielsen H B and Ninomiya M 1981 *Nucl. Phys. B* **185** 20
- [4] Lüscher M 1998 *Phys. Lett. B* **428** 342
- [5] Hasenfratz P, Laliena V and Niedermayer F 1998 *Phys. Lett. B* **427** 125
- [6] Fukaya H *et al.* 2007 *Phys. Rev. Lett.* **98** 172001; 2007 *Phys. Rev. D* **76** 054503
- [7] Lüscher M 2010 *JHEP* **1008** 071; 2010 *PoS(LATTICE2010)* 015

- [8] Bietenholz W, Hip I, Shcheredin S and Volkholz J 2011 *arXiv:1109.2649 [hep-lat]*
- [9] Bietenholz W 1999 *Eur. Phys. J. C* **6** 537; Bietenholz W and Hip I 2000 *Nucl. Phys. B* **570** 423;
Bietenholz W 2002 *Nucl. Phys. B* **644** 223; Bietenholz W and Shcheredin S 2006 *Nucl. Phys. B* **754** 17
- [10] Neuberger H 1998 *Phys. Lett. B* **417** 141; 1998 *Phys. Lett. B* **427** 353
- [11] Schwinger J 1962 *Phys. Rev.* **128** 2425
- [12] Coleman S R, Jackiw R and Susskind L 1975 *Annals Phys.* **93** 267
- [13] Smilga A V 1997 *Phys. Rev. D* **55** 443
- [14] Coleman S R 1976 *Annals Phys.* **101** 239
- [15] Bietenholz W, Jansen K and Shcheredin S 2003 *JHEP* **0307** 033
- [16] Del Debbio L, Giusti L and Pica C 2005 *Phys. Rev. Lett.* **94** 032003
Dürr S, Fodor Z, Hoelbling C and Kurth T 2007 *JHEP* **0704** 055
- [17] Dürr S 2001 *Nucl. Phys. B* **611** 281
- [18] Dürr S and Hoelbling C 2005 *Phys. Rev. D* **71** 054501
- [19] Aoki S, Fukaya H, Hashimoto S and Onogi T 2007 *Phys. Rev. D* **76** 054508
- [20] Aoki S *et al.* (JLQCD and TWQCD Collaborations) 2008 *Phys. Lett. B* **665** 294
- [21] Brower R, Chandrasekharan S, Negele J W and Wiese U-J 2003 *Phys. Lett. B* **560** 64
- [22] Kaplan D B 1992 *Phys. Lett. B* **288** 342
- [23] Hasenfratz P 1998 *Nucl. Phys. B* **525** 401
- [24] Lüscher M and Schaefer S 2011 *JHEP* **1107** 036